CHIN. PHYS. LETT. Vol. 34, No. 5 (2017) 057302 **Express Letter**

Two-Dimensional Node-Line Semimetals in a Honeycomb-Kagome Lattice *

Jin-Lian Lu(卢金炼)[1†], Wei Luo(罗伟)[2,3†], Xue-Yang Li(李雪阳)[2], Sheng-Qi Yang(杨晟祺)[2], Jue-Xian Cao(曹觉先)[1], Xin-Gao Gong(龚新高)[2,3], Hong-Jun Xiang(向红军)[2,3**]

[1] *Department of Physics, Xiangtan University, Xiangtan 411105*
[2] *Key Laboratory of Computational Physical Sciences (Ministry of Education), State Key Laboratory of Surface Physics, and Department of Physics, Fudan University, Shanghai 200433*
[3] *Collaborative Innovation Center of Advanced Microstructures, Nanjing 210093*

(Received 24 March 2017)

Recently, the concept of topological insulators has been generalized to topological semimetals, including three-dimensional (3D) Weyl semimetals, 3D Dirac semimetals, and 3D node-line semimetals (NLSs). In particular, several compounds (e.g., certain 3D graphene networks, Cu_3PdN, Ca_3P_2) were discovered to be 3D NLSs, in which the conduction and valence bands cross at closed lines in the Brillouin zone. Except for the two-dimensional (2D) Dirac semimetal (e.g., graphene), 2D topological semimetals are much less investigated. Here we propose a new concept of a 2D NLS and suggest that this state could be realized in a new mixed lattice (named as HK lattice) composed by Kagome and honeycomb lattices. It is found that A_3B_2 (A is a group-IIB cation and B is a group-VA anion) compounds (such as Hg_3As_2) with the HK lattice are 2D NLSs due to the band inversion between the cation Hg-s orbital and the anion As-p_z orbital with respect to the mirror symmetry. Since the band inversion occurs between two bands with the same parity, this peculiar 2D NLS could be used as transparent conductors. In the presence of buckling or spin-orbit coupling, the 2D NLS state may turn into a 2D Dirac semimetal state or a 2D topological crystalline insulating state. Since the band gap opening due to buckling or spin-orbit coupling is small, Hg_3As_2 with the HK lattice can still be regarded as a 2D NLS at room temperature. Our work suggests a new route to design topological materials without involving states with opposite parities.

PACS: 73.20.At, 71.55.Ak, 71.20.−b DOI: 10.1088/0256-307X/34/5/057302

Due to the unique band structure, topological insulators (TIs) have drawn broad attention in recent years.[1–4] They have a bulk energy gap between the valence and conduction bands, which is similar to ordinary insulators but contains a nontrivial gapless boundary state that is inspired by their bulk topological states. Similar to TIs, a new topological state of metals has been proposed. In topological semimetals, the valence and conduction bands cross near the Fermi level to form band touch points and exhibit new topological quantum states. Up to date, according to the property of band touch points, three-dimensional (3D) topological semimetals have been divided into three kinds, i.e., Dirac semimetal (DSM) and Weyl semimetal (WSM) that possesses discrete band touch points, and node-line semimetal (NLS) in which the band touch points form a closed ring in momentum space. Wan *et al.* first proposed that pyrochlore iridates (such as $Y_2Ir_2O_7$) are magnetic WSMs in which the time-reversal symmetry is broken.[5] Subsequently, Xu *et al.* have proposed that ferromagnetic $HgCr_2Se_4$ possesses a single pair of Weyl fermions with opposite chiralities separated in momentum space.[6] Spatial inversion broken WSM state was also discovered in nonmagnetic materials including TaAs, TaP, NbAs and NbP.[2,7–11] When two opposite chiral Weyl fermions meet, the DSM state with a four-fold degenerate Dirac node protected by both inversion and time-reversal symmetries may appear. Na_3Bi[12,13] and Cd_3As_2[14–18] have been predicted theoretically and verified experimentally to be 3D DSM semimetals.

In 2011, Burkov *et al.* proposed the concept of 3D NLS with broken time-reversal symmetry and gave an explicit model realization of 3D NLSs in a normal insulator-TI superlattice structure.[19] The 3D NLS state was recently extended to the case of time-reversal invariant systems.[20,21] Three-dimensional carbon allotrope materials with a negligible SOC effect such as Mackay–Terrones crystals,[20] hyperhoneycomb lattices,[22] and the interpenetrated graphene network[23] were proposed to be time-reversal invariant 3D NLSs. In addition, the cubic antiperovskite materials Cu_3PdN,[24,25] Ca_3P_2,[26,27] noncentrosymmetric superconductors $PbTaSe_2$[28] and $TlTaSe_2$[29] were also predicted to display such exotic states. There are drumhead-like surface flat bands on the surface of 3D NLSs. When SOC is taken into account, each node-line ring may drive into a pair of Dirac nodes or Weyl nodes.[24,25]

In contrast to the case of 3D topological semimetals for which a comprehensive understanding is now achieved, the research field of 2D topological semimetals is still under development. When the SOC effect is neglected, graphene can be seen as a 2D Dirac semimetal.[30] Young and Kane proposed the existence of three possible distinct 2D Dirac semimetal phases by using a two-site tight binding model.[31] A Lieb lattice with intra-unit-cell and suitable nearest-

*Supported by the National Natural Science Foundation of China under Grant No 11374056, the Special Funds for Major State Basic Research under Grant No 2015CB921700, the Program for Professor of Special Appointment (Eastern Scholar), the Qing Nian Ba Jian Program, and the Fok Ying Tung Education Foundation.
†Jin-Lian Lu and Wei Luo contributed equally to this work.
**Corresponding author. Email: hxiang@fudan.edu.cn

neighbor hopping terms between the spinless fermions was proposed to be a 2D Chern semimetal with a single Dirac-like point.[32] Recently, Wang *et al.* found a 2D NLS-like state in graphene on WS_2 due to the strong interface-induced spin-orbit interaction, but they did not discuss the importance and the implication of the unique 2D NLS deeply.[33] Here we will first propose a concept of the 2D NLS and discover some corresponding materials.

In the present work, based on effective model analysis and first-principles calculations, we put forward a new concept of the 2D NLS and show that this novel state can be realized in a new composite lattice (hereafter referred to as the HK lattice) with interpenetrating Kagome and honeycomb lattices. Furthermore, first-principles calculations show that a series of compounds (e.g, Hg_3As_2) with the HK lattice are indeed 2D NLSs in which the band inversion happens between the Hg-s orbital and the As-p_z orbital. When considering SOC, a tiny band gap at the node-line ring can be induced, resulting in a novel topological crystalline insulator (TCI) without parity inversion.

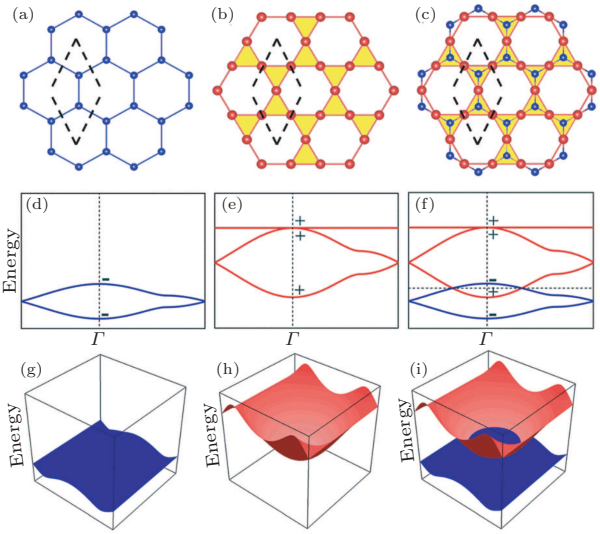

Fig. 1. The 2D node-line semimetal in the honeycomb-Kagome lattice. (a)–(c) The geometrical structures of the honeycomb, kagome, and honeycomb-Kagome (HK) lattices, and (d)–(f) the 2D band structures of honeycomb, Kagome, and HK lattices, respectively. (g)–(i) The corresponding 3D band structures. The dashed lines show the unit cell. The x-axis is along the direction of a lateral lattice vector. There is a p_z (s) orbital on each honeycomb (kagome) lattice point. The band structures are computed with $E_p = -4.6$, $t_p = 0.3$ for the honeycomb lattice and $E_s = -1.8$, $t_s = 0.6$ for the kagome lattice. Here $+$ and $-$ in (d)–(f) denote the eigenvalues of the electronic states with respect to the x–y mirror plane.

It is well known that the band crossing in a 2D system could happen at a special point in the 2D Brillouin zone. For example, the π and π^* bands in graphene cross each other to form Dirac points at high symmetry points K and K'. Here we will address an interesting question whether the touching points can form a node-ring in a 2D system. For simplicity, we consider the spinless case (without the SOC effect). If two bands happen to cross each other at a k-point, there are two possibilities: either these two bands belong to two different one-dimensional irreducible representations, or they together form the basis of a two-dimensional irreducible representation. Among the k-points of a node-ring in the 2D Brillouin zone, some of them must be general k-points with the lowest point group symmetry. In the 3D case, a general k-point can only have the C_1 point group symmetry. In contrast, a general k-point in the 2D case could have the Cs point group symmetry if the 2D system has an in-plane mirror (or glide mirror) symmetry. Since the Cs point group only has two one-dimensional irreducible representations (A' and A''), the two bands in a 2D NLS must belong to A' and A'' representations, respectively. Therefore, to realize a 2D NLS, the material should have an in-plane mirror (or glide mirror) symmetry and the two bands near the Fermi level should transform differently under the mirror symmetry.

We find that the 2D NLS state may be present in a composite lattice (i.e., HK lattice) with interpenetrating Kagome and honeycomb lattices. Let us start from the simple tight-binding model of a honeycomb lattice. In Fig. 1(a), we show the top view of a planar honeycomb lattice with the D_{6h} point group. There are two sites per primitive cell and each site is associated with a p_z orbital. For simplicity, we only consider the nearest neighboring (NN) interaction. Similar to the graphene case, we can obtain the eigenvalues of two bands with

$$E_{1,2} = E_p \pm t_p[3 + 2\cos(2k_x) + 2\cos(k_x + \sqrt{3}k_y) + 2\cos(\sqrt{3}k_y - k_x)]^{1/2},$$

where E_p and t_p are the on-site energies of the p_z orbital and the hopping between NN p_z orbitals, respectively. It is well-known that there are Dirac points (K and K') in the band structure (see Fig. 1(d)).[30] Another interesting observation from the expression of the eigenvalues is that the upper (lower) anti-bonding (bonding) band has the maximum (minimum) at Γ. For the Kagome lattice (see Fig. 1(b)), there are three sites in the primitive cell. Each site has one s orbital and only the NN interaction is taken into consideration. The eigenvalues of the three bands are

$$E_1 = E_s - 2t_s,$$
$$E_{2,3} = \mp t_s[3 + 2\cos(2k_x) + 2\cos(k_x + \sqrt{3}k_y) + 2\cos(\sqrt{3}k_y - k_x)]^{1/2} + t_s + E_s,$$

where E_s and t_s are the on-site energies of the s orbital and the NN hopping parameter (negative for the s orbital), respectively. The topmost band (see Fig. 1(e)) is flat, which is characteristic for the Kagome lattice.[34,35] The other two lower bands have the same dispersion as the honeycomb lattice. Thus the bottom of the lowest-energy band locates at Γ. We now combine the Kagome lattice with the honeycomb lattice to form the HK lattice (see Fig. 1(c)). The HK lattice has a spatial inversion symmetry with a D_{6h}

point group symmetry. Since the s orbital and p_z orbital are symmetric or anti-symmetric with respect to the x–y mirror plane, there is no interaction between s and p_z orbitals. Thus the band structure of the HK lattice will be simply the superimposition of the band structures of the Kagome and honeycomb lattices. If the bottommost band of the Kagome lattice has an energy lower than the topmost band of the honeycomb lattice at Γ, there will be band inversion between the s and p_z bands in the HK lattice (see Fig. 1(f)) and its 3D band structure can be seen in Figs. 1(g)–1(i). We consider the case that two of the five bands are filled. Note that these two states close to the Fermi level have even parity, suggesting that the band inversion has a different meaning from the usual band inversion that happens between bands with opposite parities. Since the s band and p_z band are even or odd with respect to the x–y mirror plane, the band crossing points will form a closed node-line ring. Thus the 2D NLS state due to the presence of the mirror symmetry may be realized in the HK lattice.

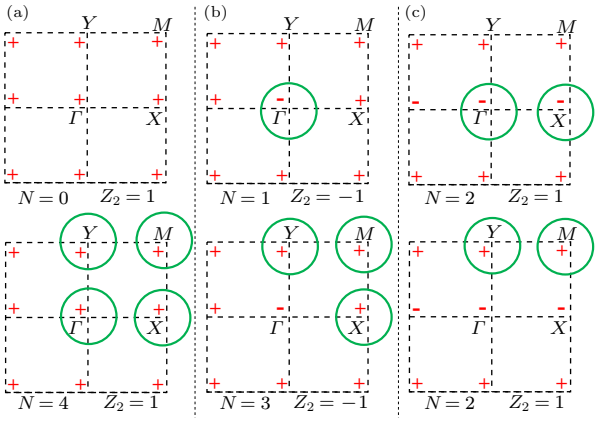

Fig. 2. Schematic illustration of the representative cases which prove $Z_2 = \xi_\Gamma\xi_X\xi_Y\xi_M = (-1)^N$, where N is the number of node-rings, + and − denote the eigenvalues of the electronic states with respect to the x–y mirror plane.

Since the Z_2 number[24] based on the Berry phase for the 3D NLS cannot be defined in the 2D case, we propose to use the mirror eigenvalues to define the Z_2 number that characterizes the 2D node-line semimetal. This provides a way to characterize whether the 2D node-line semimetal has an even or odd number of node-rings. In a 2D spinless system with the time reversal symmetry, $\Gamma[(0,0)]$, $X[(0.5,0)]$, $Y[(0,0.5)]$ and $M[(0.5,0.5)]$ are the four time-reversal invariant points. We assume that there is a lateral mirror plane in this 2D system. Therefore, each state for any k-point in the Brillouin zone can have a definite mirror eigenvalue $\xi = +1$ or -1. The Z_2 number that characterizes the total number (N) of node lines in a 2D system can be defined as $Z_2 = \xi_\Gamma\xi_X\xi_Y\xi_M$, where $\xi_a = \prod_{n=1}^{N_{\rm occ}} \xi_{\rm an}$ ($N_{\rm occ}$ is the number of the occupied states). One can easily prove that $Z_2 = (-1)^N$. Firstly, if there is a node line centered at $\boldsymbol{K}$ that is not time-reversal invariant, there must be another node line centered at $-\boldsymbol{K}$. Therefore, we only need to consider the case that the node lines are centered at time-reversal invariant points. As shown in Fig. 2(a), when all the mirror eigenvalues at the four time-reversal invariant points are $+1$, the number of node lines could be 0 or 4. This is in agreement with the relationship that $Z_2 = \xi_\Gamma\xi_X\xi_Y\xi_M = (-1)^N$. In the other two cases (Figs. 2(b) and 2(c)), it can be easily seen that $Z_2 = \xi_\Gamma\xi_X\xi_Y\xi_M = (-1)^N$ is also satisfied. If we reverse all the mirror eigenvalues, the same picture will remain. Therefore, we have proved $Z_2 = (-1)^N$, i.e., the number of the node-ring is even (odd) when $Z_2 = \xi_\Gamma\xi_X\xi_Y\xi_M$ is $+1$ (-1). In the case of planar Hg_3As_2, $N = 1$ and $Z_2 = -1$.

In the following we will design 2D NLS materials based on the HK A_3B_2 lattice. To obtain a 2D NLS state in an HK lattice, the valence band and conduction band should be contributed by p_z and s states, respectively. In usual compounds, the occupied p state and empty s state originates from the anion and cation, respectively. Therefore, the honeycomb B-sites should be anions, while the Kagome A-sites should be cations. Since the -6 valence state of an anion is rare, the valence states of A-cation and B-anion of a stable A_3B_2 compound should be $+2$ and -3, respectively. After extensive tests, we find that if the A-cation is a group-IIB element (e.g., Zn, Cd and Hg) and B-anion is a group VA element (e.g., N, P, As, Sb and Bi), the A_3B_2 compound may be a 2D NLS. With first principle calculations, we obtain the relaxed structures and find that the 2D NLS state can be present in five A_3B_2 compounds (i.e., Zn_3Bi_2, Cd_3Bi_2, Hg_3As_2, Hg_3Sb_2 and Hg_3Bi_2). In addition, although planar Cd_3As_2 with the relaxed structure is a normal semiconductor, it becomes a 2D NLS when 1% tensile strain is applied. As can be seen from the band structures of these compounds (see Fig. S1 in the supplemental materials), there are two bands crossing each other near Γ at the Fermi level. The fat band representation clearly shows that the conduction band is contributed by the s orbital of the cation and the valence band is contributed by the p_z orbital of the anion. It is found that the degree of the band inversion increases when cation and anion become heavier. For example, the inversed energies of the Hg system are 0.841, 0.982 and 1.127 eV for Hg_3As_2, Hg_3Sb_2 and Hg_3Bi_2, respectively. This is because the s level decreases with the atomic number of the cation element, while the p level increases with the atomic number of the anion element. Since the local density approximation usually underestimates the band gap (see Fig. 3(a)), we adopt a more reliable hybrid functional HSE06 to confirm that Hg_3As_2 is still a 2D NLS (see Fig. S2). Interestingly, we find that the optical absorption of HK Hg_3As_2 below 2 eV is very weak (see Fig. S3). This is because both VBM and CBM states have even parity, thus the direct optical transition between them is forbidden. Due to the linear band dispersion near the node-line ring, the conductivity in HK Hg_3As_2 is expected to be rather high. This suggests that 2D NLS can be a promising candidate for transparent conductors in touch screens and solar cells.[36,37]

So far, the effect of SOC is neglected. After inclu-

ding the SOC in the density functional calculations, a small band gap will be opened around the node-line ring. We can understand this from the symmetry analysis. One only needs to check whether the gap will be opened along the two high-symmetry lines starting from Γ (i.e., $\Gamma \to K$ and $\Gamma \to M$). For the k-points on the two lines (except for the end points), the symmetry group is the double group of C_{2v}. Since the double group of C_{2v} only has a 2D irreducible representation Γ_5, both the CBM and VBM states must belong to the same irreducible representation Γ_5 and they could interact with each other, resulting in a band gap opening. For Hg_3As_2, the band gap is 34 meV (see Fig. 3(b)), and the SOC-induced band gaps are 65.9, 80.1, 24.8 and 100.2 meV for Zn_3Bi_2, Cd_3Bi_2, Hg_3Sb_2 and Hg_3Bi_2, respectively. This value is smaller than the SOC-induced gap opening (about 62 meV) in a 3D NLS system Cu_3NPd.[24] Note that the SOC-induced band gap opening can be tuned by changing the elements. For example, the SOC-induced band gap in Cd_3As_2 with 1% tensile strain is only 0.2 meV. Since the SOC-induced band gap opening in HK A_3B_2 compounds is small, we can still regard them as 2D NLSs at room temperature, similar to the 3D NLS case.

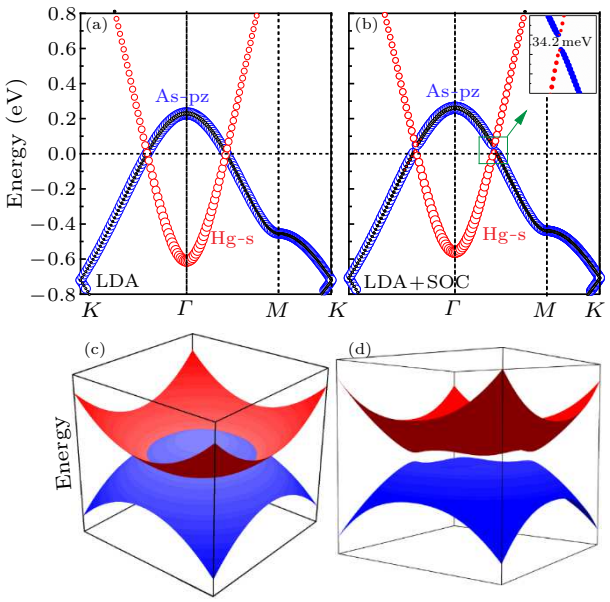

Fig. 3. Band structures of planar Hg_3As_2 with the HK lattice. (a, b) The 2D band structures calculated by LDA and LDA+SOC, respectively. (c, d) The corresponding 3D band structures from the $k \cdot p$ theory. In (c), $C_0 = -1$, $C_1 = 1$, $M_0 = -1$ and $M_1 = 1$ are employed. In addition to these parameters, a large value (0.5) for A_0 is adopted in (d) for clarity.

To gain more insight into the origin of the 2D NLS and SOC-induced gap opening in A_3B_2 compounds, we construct the effective $k \cdot p$ Hamiltonian with the invariant method.[39] To be more specific, we consider Hg_3As_2 as a typical example. According to the LDA calculation (without SOC), the VBM and CBM states at Γ are mainly contributed by Hg $|s\rangle$ and As $|p_z\rangle$ orbitals, respectively. The VBM state is a bonding state between the three Hg s orbitals, while the CBM state is an anti-bonding state between the As p_z orbitals,

$$|S^+\rangle = \frac{1}{\sqrt{3}}(|\mathrm{Hg}_1, s\rangle + |\mathrm{Hg}_2, s\rangle + |\mathrm{Hg}_3, s\rangle),$$
$$|P_z^+\rangle = \frac{1}{\sqrt{2}}(|\mathrm{As}_1, p_z\rangle - |\mathrm{As}_2, p_z\rangle),$$

where the + sign indicates that both states have even parity. The irreducible representations of $|S^+\rangle$ and $|P_z^+\rangle$ are Γ_1^+ and Γ_3^+ of D_{6h}, respectively. We will use $|S^+\rangle$ and $|P_z^+\rangle$ as the bases to construct a low-energy effective Hamiltonian around the Γ point. The effective Hamiltonian obtained from the invariant method reads

$$H(k) = \begin{bmatrix} \varepsilon(k) + M(k) & 0 \\ 0 & \varepsilon(k) - M(k) \end{bmatrix},$$

where $\varepsilon(k) = C_0 + C_1(k_x^2 + k_y^2)$ and $M(k) = M_0 + M_1(k_x^2 + k_y^2)$. It is clear that these two states are decoupled with the eigenvalues $E(k) = C_0 \pm M_0 + (C_1 \pm M_1)(k_x^2 + k_y^2)$. It can be seen that if $M_0 M_1 > 0$, the system is a normal insulator. Otherwise, a band inversion takes place. In this case, the two bands will cross each other at the k-points which satisfy $k_x^2 + k_y^2 = -M_0/M_1$. This means that the crossing points form a node-line ring (see Fig. 3(c)), in agreement with the first-principles result. Our $k \cdot p$ analysis shows that the SOC-induced gap opening is due to the quadratic term of k instead of the linear term (see part 2 of the supplemental materials).

We find that the insulating state of Hg_3As_2 with the HK lattice induced by the SOC is a 2D TCI state.[38,40] Qualitatively, this can be understood by examining the band structure without considering SOC. From the LDA band structure, band inversion only takes place at the Γ point instead of on the other three time-reversal points. Note that here the meaning of 'band inversion' is different from that in the field of topological insulators. In the latter case, the band inversion usually means inversion between eigenstates with opposite parities, while in our context, both eigenstates (s and p_z states) have the same even parity but opposite eigenvalues with respect to the x–y mirror plane. Since the band inversion relating to the mirror symmetry occurs only once, it is expected that the system will become a 2D TCI state after a band gap is opened by SOC. Interestingly, the band inversion mechanism in our case is different from the case in monolayer IV–VI (e.g., PbSe) where the TCI behavior is due to the band inversion with respect to both spatial inversion and the x–y mirror plane at X and Y points.[28,41,42] We support our above argument by numerically computing the mirror Chern number with a Slater–Koster TB model. We find that Hg_3As_2 has a non-zero mirror Chern number of 2, suggesting that it is a TCI after SOC is considered. We further confirm this result by computing the edge states of the semi-infinite Hg_3As_2 nanoribbons with both armchair and zigzag terminations. The recursive method is adopted to compute the surface local density of states.[43]

Since the presence of the edges does not break the mirror symmetry with respect to the x–y plane, it is expected that there will exist nontrivial helical edge states as a characteristic feature of TCI.[44,45] This is indeed the case. As can be seen from Fig. 4 for the armchair ribbon and the zigzag ribbon case, there are two helical edge states within the bulk band gap for different terminations. The number of the edge states is in agreement with the calculated mirror Chern number.

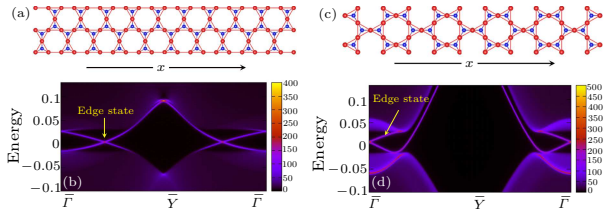

Fig. 4. The edge states of armchair and zigzag ribbon of Hg_3As_2 with the HK lattice. (a, c) The geometrical structures. (b, d) Energy and momentum-dependent local density of states of the semi-infinite armchair and zigzag ribbons computed with the Green function method. The SOC effect has been included.

Finally, we consider the effect of possible buckling on the electronic structure of the A_3B_2 compounds with the HK lattice. It is found that the gap induced by the buckling is too small so that HK Hg_3As_2 with a small buckling can still be regarded as a 2D NLS at room temperature (see part 3 of the supplemental materials).

In summary, we have proposed for the first time the concept of the 2D NLS. A newly constructed HK lattice is predicted to display the 2D NLS behavior due to the band inversion with respect to the mirror symmetry. It is predicted that this 2D NLS state can be realized in the real A_3B_2 (A is a group-IIB cation and B is a group-VA anion) compound (such as Hg_3As_2) with the HK lattice.

We thank Dr. Rui Yu and Dr. Hongming Weng for our useful discussions.

References

[1] Hasan M Z and Kane C L 2010 *Rev. Mod. Phys.* **82** 3045
[2] Lv B Q, Muff S, Qian T, Song Z D, Nie S M, Xu N, Richard P, Matt C E, Plumb N C, Zhao L X, Chen G F, Fang Z, Dai X, Dil J H, Mesot J, Shi M, Weng H M and Ding H 2015 *Phys. Rev. Lett.* **115** 217601
Liu C C, Feng W X and Yao Y G 2011 *Phys. Rev. Lett.* **107** 076802
[3] Fu L and Kane C L 2007 *Phys. Rev.* B **76** 045302
[4] Bernevig B A, Hughes T L and Zhang S C 2006 *Science* **314** 1757
[5] Wan X, Turner A M, Vishwanath A and Savrasov S Y 2011 *Phys. Rev.* B **83** 205101
[6] Xu G, Weng H, Wang Z, Dai X and Fang Z 2011 *Phys. Rev. Lett.* **107** 186806
[7] Weng H, Fang C, Fang Z, Bernevig B A and Dai X 2015 *Phys. Rev.* X **5** 011029
[8] Lv B Q, Weng H M, Fu B B, Wang X P, Miao H, Richard J Ma P, Huang X C, Zhao L X, Chen G F, Fang Z, Dai X, Qian T and Ding H 2015 *Phys. Rev.* X **5** 031013
[9] Xu N, Weng H M, Lv B Q, Matt C, Park J, Bisti F, Strocov V N, Gawryluk D, Pomjakushina E, Conder K, Plumb N C, Radovic M, Autès G, Yazyev O V, Fang Z, Dai X, Aeppli G, Qian T, Mesot J, Ding H and Shi M 2016 *Nat. Commun.* **7** 11006
[10] Xu S Y, Belopolski I, Daniel S S, Zhang C, Chang G, Guo C, Bian G, Yuan Z, Lu H, Chang T R, Shibayev P P, Prokopovych M L, Alidoust N, Zheng H, Lee C C, Huang S M, Sankar R, Chou F C, Hsu C H, Jeng H T, Bansil A, Neupert T, Strocov V N, Lin H, Jia S and Hasan M Z 2015 *Sci. Adv.* **1** e1501092
[11] Huang S M, Xu S Y, Belopolski I, Lee C C, Chang G, Wang B, Alidoust N, Bian G, Neupane M, Zhang C, Jia S, Bansil A, Lin H and Hasan M Z 2015 *Nat. Commun.* **6** 7373
[12] Liu Z K, Zhou B, Zhang Y, Wang Z J, Weng H M, Prabhakaran D, Mo S K, Shen Z X, Fang Z, Dai X, Hussain Z and Chen Y L 2014 *Science* **343** 864
[13] Wang Z, Sun Y, Chen X Q, Franchini C, Xu G, Weng H, Dai X and Fang Z 2012 *Phys. Rev.* B **85** 195320
[14] Liu Z K, Jiang J, Zhou B, Wang Z J, Zhang Y, Weng H M, Prabhakaran D, Mo S K, Peng H, Dudin P, Kim T, Hoesch M, Fang Z, Dai X, Shen Z X, Feng D L, Hussain Z and Chen Y L 2014 *Nat. Mater.* **13** 677
[15] He L P, Hong X C, Dong J K, Pan J, Zhang Z, Zhang J and Li S Y 2014 *Phys. Rev. Lett.* **113** 246402
[16] Neupane M, Xu S Y, Sankar R, Alidoust N, Bian G, Liu C, Belopolski I, Chang T R, Jeng H T, Lin H, Bansil A, Chou F and Hasan Z M 2014 *Nat. Commun.* **5** 3786
[17] Pariari A, Dutta P and Mandal P 2015 *Phys. Rev.* B **91** 155139
[18] Wang Z, Weng H, Wu Q, Dai X and Fang Z 2013 *Phys. Rev.* B **88** 125427
[19] Burkov A A, Hook M D and Balents L 2011 *Phys. Rev.* B **84** 235126
[20] Weng H, Liang Y, Xu Q, Yu R, Fang Z, Dai X and Kawazoe Y 2015 *Phys. Rev.* B **92** 045108
[21] Fang C, Chen Y, Kee H Y and Fu L 2015 *Phys. Rev.* B **92** 081201
[22] Mullen K, Uchoa B and Glatzhofer D T 2015 *Phys. Rev. Lett.* **115** 026403
[23] Chen Y, Xie Y, Yang S A, Pan H, Zhang F, Cohen M L and Zhang S 2015 *Nano Lett.* **15** 6974
[24] Kim Y, Wieder B J, Kane C L and Rappe A M 2015 *Phys. Rev. Lett.* **115** 036806
[25] Yu R, Weng H, Fang Z, Dai X and Hu X 2015 *Phys. Rev. Lett.* **115** 036807
[26] Xie L S, Schoop L M, Seibel E M, Gibson Q D, Xie W and Cava R J 2015 arXiv:1504.01731v1[cond-mat.mtrl-sci]
[27] Chan Y-H, Chiu C K, Chou M Y and Schnyder A P 2015 arXiv:1510.02759v2[cond-mat.mes-hall]
[28] Bian G, Chang T R, Sankar R, Xu S Y, Zheng H, Neupert T, Chiu C K, Huang S M, Chang G, Belopolski I, Sanchez D S, Neupane M, Alidoust N, Liu C, Wang B K, Lee C C, Jeng H T, Bansil A, Chou F, Lin H and Hasan M Z 2015 arXiv:1505.03069v1[cond-mat.mes-hall]
[29] Bian G, Chang T R, Zheng H, Velury S, Xu S Y, Neupert T, Chiu C K, Huang S M, Sanchez D S, Belopolski I, Alidoust N, Chen P J, Chang G, Bansil A, Jeng H T, Lin H and Hasan M Z 2016 *Phys. Rev.* B **93** 121113(R)
[30] Castro Neto A H et al 2009 *Rev. Mod. Phys.* **81** 109
[31] Young S M and Kane C L 2015 *Phys. Rev. Lett.* **115** 126803
[32] Palumbo Gand Meichanetzidis K 2015 *Phys. Rev.* B **92** 235106
[33] Wang Z et al 2015 *Nat. Commun.* **6** 8339
[34] Guo H M and Franz M 2009 *Phys. Rev.* B **80** 113102
[35] Heikkilä T T and Volovik G E 2015 arXiv:1504.05824v1[cond-mat.mtrl-sci]
[36] Chopra K L, Major S and Pandya D K 1983 *Thin Solid Films* **102** 1
[37] Bonaccorso F et al 2010 *Nat. Photon.* **4** 611
[38] Fu L 2011 *Phys. Rev. Lett.* **106** 106802
[39] Liu C X et al 2010 *Phys. Rev.* B **82** 045122
[40] Liu J et al 2013 *Nat. Mater.* **13** 178
[41] Wrasse E O and Schmidt T M 2014 *Nano Lett.* **14** 5717
[42] Liu J, Qian X and Fu L 2015 *Nano Lett.* **15** 2657
[43] López Sancho M P et al 1985 *J. Phys.* F **15** 851
[44] Liu J and Vanderbilt D 2014 *Phys. Rev.* B **90** 155316
[45] Voon L C L Y and Willatzen M 2009 *The kp Method: Electronic Properties of Semiconductors* (New York: Springer)

Supplemental materials for

Two-dimensional node-line semimetals in a honeycomb-kagome lattice

Jin-Lian Lu(卢金炼)[1], Wei Luo(罗伟)[2,3], Xue-Yang Li(李雪阳)[2], Sheng-Qi Yang(杨晟祺)[2], Jue-Xian Cao(曹觉先)[1], Xin-Gao Gong(龚新高)[2,3], Hong-Jun Xiang(向红军)*[2,3]

[1]*Department of Physics, Xiangtan University, Xiangtan, Hunan, 411105*

[2]*Key Laboratory of Computational Physical Sciences (Ministry of Education), State Key Laboratory of Surface Physics, and Department of Physics, Fudan University, Shanghai 200433*

[3]*Collaborative Innovation Center of Advanced Microstructures, Nanjing 210093*

J.L. L. and W. L. contributed equally to this work.

**E-mail: hxiang@fudan.edu.cn*

1. Computational details

DFT calculations. In our work, density functional theory (DFT) method is used for structural relaxation and electronic structure calculation. The ion-electron interaction is treated by the projector augmented-wave[1] technique as implemented in the Vienna ab initio simulation package[2]. The exchange-correlation potential is treated by LDA.[3,4] For structural relaxation, all the atoms are allowed to relax until atomic forces are smaller than 0.01 eV/Å. The HSE06 functional[5] is adopted to compute the accurate band structure of planar HK Hg_3As_2.

PSO Algorithm for Q2D Systems. With our newly developed global optimization PSO approach,[6,7] we search the lowest-energy structure of Hg_3As_2 with the thickness less than 0.8 Å. Our implementation has been described elsewhere.[6] In the PSO simulation[8] for the Hg_3As_2 system, we set the population size to 30 and the number of generations to 20. We consider four different initial thickness (0Å, 0.5 Å, 1.0 Å, 1.5 Å) for each system. In addition, we repeat twice of each calculation in order to make results reliable.

Invariant method for deriving the effective Hamiltonian. The invariant method[9]

is adopted to obtain the low-energy effective Hamiltonian of HK Hg_3As_2 near Γ. First, we analyze the symmetry of the VBM and CBM states of Hg_3As_2 to find out the corresponding irreducible representations. Then, we classify basis matrices and functions of the finite wave vector **k** according to the irreducible representations of the point-group of Hg_3As_2. The double-valued D_{6h} point group is used when SOC is included. Finally, one construct the model Hamiltonian by combining the basis matrix and functions of **k** according to their symmetry properties. Through diagonalizing this Hamiltonian, one can get the eigenvalues of electronic states of Hg_3As_2.

.

2. Effect of spin-orbit coupling on the electronic structure of the planar HK lattice from the $k \cdot p$ theory

In the case of SOC, we have four basis functions, namely, $\left|S^+\uparrow\right\rangle,\left|P_z^+\uparrow\right\rangle,\left|S^+\downarrow\right\rangle,\left|P_z^+\downarrow\right\rangle$. $\left|S^+\uparrow,\downarrow\right\rangle$ and $\left|P_z^+\uparrow,\downarrow\right\rangle$ belong to 2D Γ_7^+ and Γ_8^+ irreducible representations of double group of D_{6h}, respectively. Here, besides the point group symmetry, time reversal symmetry is also taken into account to derive the effective Hamiltonian up to the third order of **k** around Γ:

$$H(k)=\begin{bmatrix} \varepsilon(k)+M(k) & 0 & 0 & B(k) \\ 0 & \varepsilon(k)-M(k) & -B(k) & 0 \\ 0 & -B(k)^* & \varepsilon(k)+M(k) & 0 \\ B(k)^* & 0 & 0 & \varepsilon(k)-M(k) \end{bmatrix},$$

where $B(k)=A_0\left[i\left(k_x^2-k_y^2\right)-k_xk_y\right]$ (A_0 characterizes the magnitude of the SOC effect). It is interesting to see that the effective Hamiltonian does not contain the linear term and third order term of **k** because the basis functions have the same parity. This is different from the case of usual topological systems in which there are linear **k** terms.[9] Due to the presence of both time-reversal and inversion symmetry, there are two double degenerate bands with eigenvalues $E(k)=\varepsilon(k)\pm\sqrt{M(k)^2+|B(k)|^2}$. Interestingly, there is no four-fold degenerate point in the whole Brillouin zone since it is impossible to satisfy $M(k)=0$ and $B(k)=0$ simultaneously, i.e., a band gap will be opened at

the node-line ring by the SOC effect (see Fig. 3d). The absence of the linear **k** terms in our Hamiltonian naturally explains the small band gaps induced by SOC.

3. Effect of buckling on the electronic structure of the HK lattice

We now check the structural stability of the A_3B_2 compounds with the HK lattice. By performing global structure optimization,[6] we find that the buckled Hg_3As_2 structure (as shown in Fig. S4a) with the HK lattice has the lowest energy among all structures with the thickness less than 0.8 Å. In the relaxed structure of buckled Hg_3As_2, Hg and As atoms locate at two planes with a distance of 0.732 Å. The computed phonon frequencies[10,11] (see Fig. S5) indicate that buckled HK Hg_3As_2 is dynamically stable. The LDA band structure shown in Fig. S4c indicates that buckled HK Hg_3As_2 is a semiconductor with a LDA direct gap of 1.629 eV. The conduction and valence bands are contributed by Hg-s orbital and As-p_z orbitals, respectively. Therefore, buckled HK Hg_3As_2 is a normal insulator instead of a 2D NLS.

It is found that the band gap of buckled HK Hg_3As_2 decreases quickly as the thickness goes thinner (see Fig. S4b). When the thickness is less than 0.3 Å, the gap closes. From the LDA band structure of HK Hg_3As_2 with a 0.3 Å buckling (see Fig. S4d), we find that the conduction and valence bands cross each other along six special paths of the momentum space, i.e., $\Gamma \to K$ and $\Gamma \to K'$, but a tiny gap (about 5 meV) is opened along other directions (e.g., $\Gamma \to M$). To further understand this, we analyze the wave function symmetries along the $\Gamma \to K$ and $\Gamma \to M$. Along the $\Gamma \to K$, the irreducible representations of CBM and VBM are A' and A'' of the Cs group, respectively. While for the $\Gamma \to M$, they belong to the same irreducible representation A' of the Cs group, resulting in a gap opening. This can be seen more clearly from the 3D band structure shown in Fig. S6. Our result suggests that a small buckling will transform the 2D NLS state of the HK lattice into a 2D Dirac semi-metal state.

An effective $k \cdot p$ Hamiltonian is derived to understand the effect of buckling on the electronic structure. In the buckled HK lattice, the cations and anions locate at two planes with different heights. Therefore, the *xy*-plane mirror symmetry in the planar HK

lattice is broken, resulting in the C_{6v} symmetry for the buckled HK lattice. Without considering the SOC effect, the effective Hamiltonian obtained from the invariant method is expressed as

$$H(k)=\begin{bmatrix} \varepsilon(k)+M(k) & (R_1-iR_2)(3k_yk_x^2-k_y^3) \\ (R_1+iR_2)(3k_yk_x^2-k_y^3) & \varepsilon(k)-M(k) \end{bmatrix},$$

where R_1 and R_2 (real) are new terms due to the presence of buckling. Note that the presence of third order terms of k results from the broken of the inversion symmetry. The expression of eigenvalues is $E=\varepsilon(k)\pm\sqrt{M(k)^2+(R_1^2+R_2^2)(3k_yk_x^2-k_y^3)^2}$. From it, we can see the presence of Dirac points at K and K', in agreement with our DFT calculations. A typical band structure of the buckled HK lattice is shown in Fig. S4d. This indicates that the node-line ring in the planar HK lattice is protected by the mirror symmetry. Therefore, we find an additional third-order term of k due to the buckling, which explains why the band gap is opened along $\Gamma\rightarrow M$, but the gap is tiny. Since the band gap opening by the buckling is small, HK Hg_3As_2 with a small buckling can still be regarded as a 2D NLS at room temperature.

We propose that the thickness of buckled HK Hg_3As_2 can be tuned by applying pressure on Hg_3As_2 sandwiched by two insulating BN monolayers. The pressure (about 9 MPa) needed for turning the normal insulating state into the 2D NLS state can be easily achieved experimentally. The band structure of the three-layer system under an external pressure of 11 MPa is shown in Fig. S7. We can see that the 2D NLS remains intact despite of the presence of BN layers since the states near the Fermi level is mainly contributed by Hg-s and As-p_z orbital.

In addition, we find that the effect of insulating substrates on the electronic structure of planar HK Hg_3As_2 is negligible (see Fig. S8). It is clear that the presence of an insulating substrate has a negligible effect on the electronic structure of planar Hg_3As_2. The band gaps arising from the mirror symmetry breaking due to the substrate are 4 meV and 4.4 meV for Al_2O_3 and BN substrates respectively. Therefore, planar Hg_3As_2 on an insulating substrate can be still be regarded as a 2D node-line semimetal at room temperature.

4. Other supplemental materials

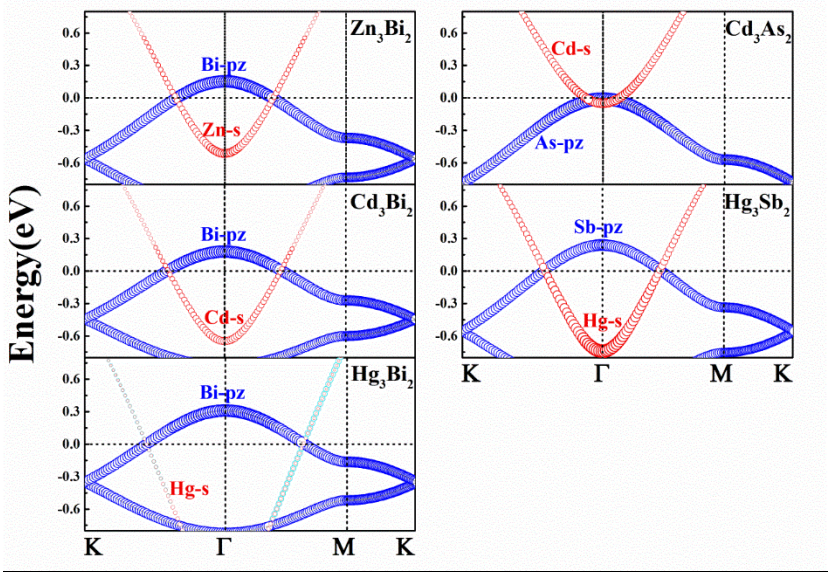

Fig. S1. LDA band structures of planar A_3B_2 compounds with the HK lattice. The lateral lattice constants of all the materials are fully relaxed except for the case of Cd_3As_2 which is under 1% tensile strain.

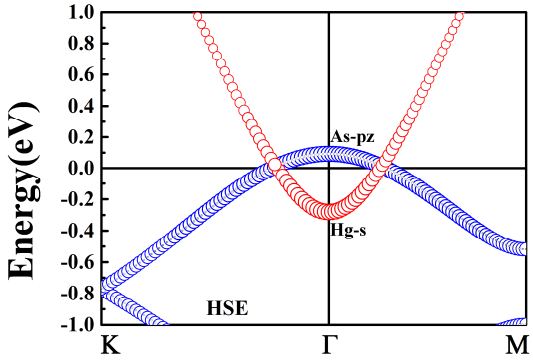

Fig. S2. Band structure of planar Hg_3As_2 with the HK lattice from the HSE06 calculation.

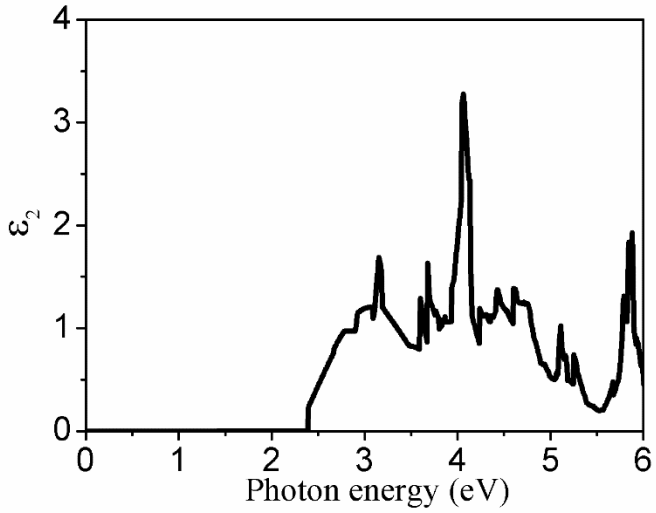

Fig. S3. Imaginary part of the dielectric constant of planar Hg_3As_2 with the HK lattice from the LDA calculation.

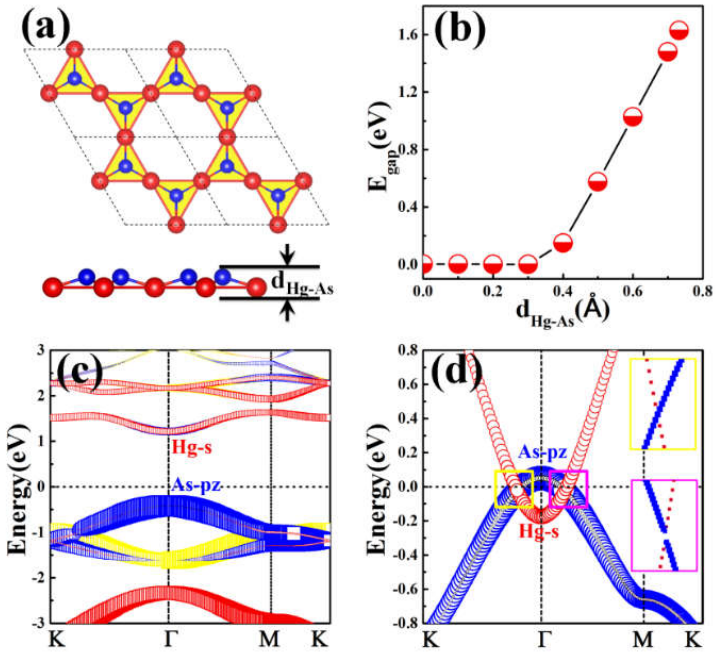

Fig. S4. Geometrical and electronic structures of buckled HK Hg_3As_2. (a) Top and side views of the structure of buckled Hg_3As_2. (b) Band gaps of buckled Hg_3As_2 as a function of thickness from the LDA calculations. (c) Band structure of the optimized structure of buckled Hg_3As_2. (d) Band structure of Hg_3As_2 with a thickness of 0.3 Å. Insets: top panel for the magnified view of the bands along the line K→Γ, bottom panel for the case of Γ→M.

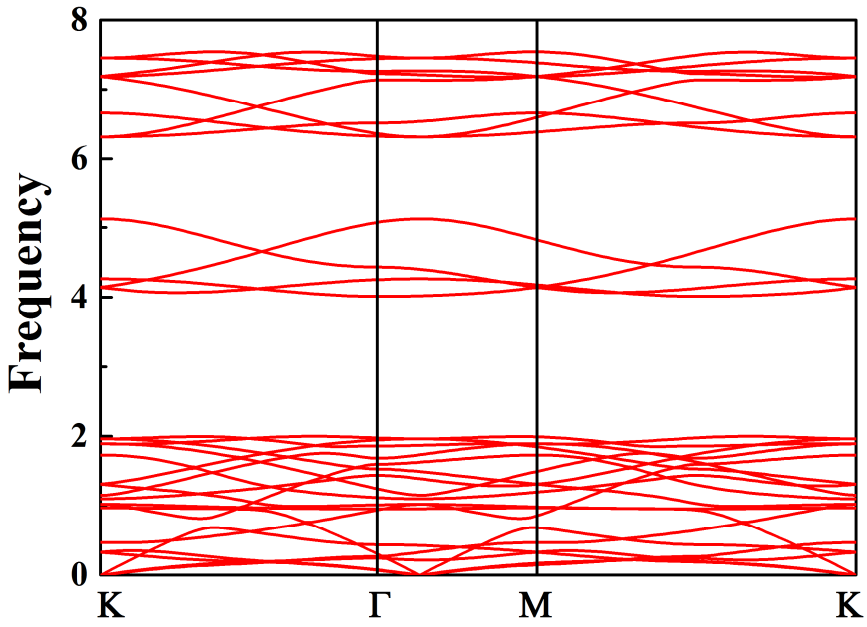

Fig. S5. Phonon dispersion of buckled Hg_3As_2 with the HK lattice. The absence of imaginary frequency indicates that the dynamic stability.

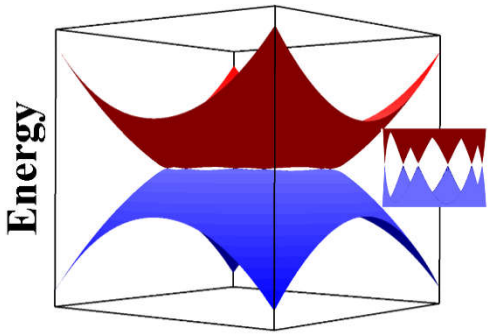

Fig. S6. 3D band structure of HK Hg_3As_2 with a 0.3 Å buckling from the $k \cdot p$ theory. The inset shows the Dirac points at K and K'. The SOC effect is ignored. $C_0 = 0, C_1 = 0, M_0 = 1, M_1 = -1, R_1 = 0.5, R_2 = 0.5$ are used for computing the band structure.

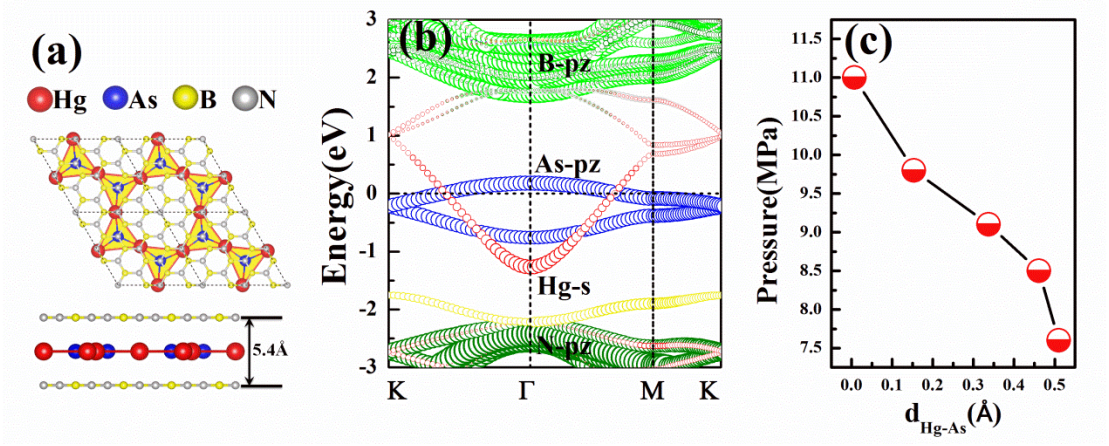

Fig. S7. Geometrical and electronic structures of Hg_3As_2 sandwiched by BN layers. (a) Top and side views of the structure of Hg_3As_2 sandwiched by BN layers. The lattice mismatch between Hg_3As_2 and BN is about 1%. (b) LDA band structure of Hg_3As_2 sandwiched by BN layer. The states near the Fermi level are contributed by Hg s orbitals and As p_z orbitals. At the Fermi level, the node-line ring can be seen (note that the band gap opening induced by the buckling is very small). (c) The required pressure applied to BN layers for obtaining the Hg_3As_2 layer with a given thickness.

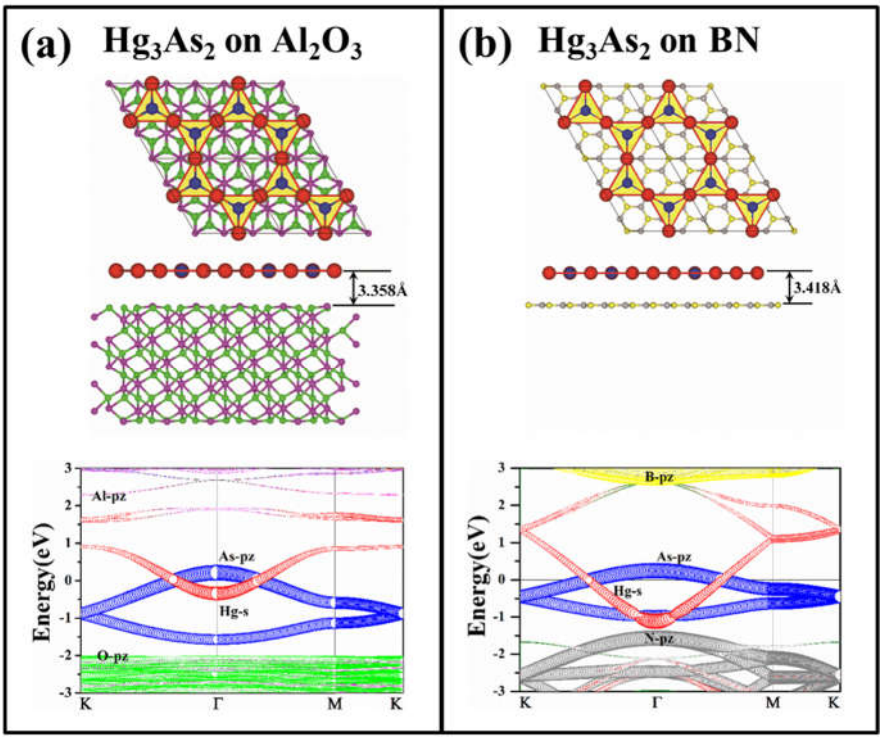

Fig. S8. Geometric and electronic band structures for planar Hg_3As_2 on (a) hexagonal Al_2O_3 [0001] surface and (b) hexagonal BN sheet.

References

[1] Blöchl P E 1994 *Phys. Rev. B* **50** 17953

[2] Kresse G and Hafner J 1994 *Phys. Rev. B* **49** 14251

[3] Ceperley D M and Alder B J 1980 *Phys. Rev. Lett.* **45** 566

[4] Perdew J P and Zunger A 1981 *Phys. Rev. B* **23** 5048

[5] Heyd J, Scuseria G E and Ernzerhof M 2003 *J. Chem. Phys.* **118** 8207

[6] Luo W, Ma Y, Gong X and Xiang H J 2014 *J. Am. Chem. Soc.* **136** 15992; Wang Y,

Lv J, Zhu L and Ma Y 2010 *Phys. Rev. B* **82** 094116

[7] Luo W and Xiang H J 2015 *Nano Lett.* **15** 3230

[8] Wang Y C, Lv J, Zhu L and Ma Y M 2010 *Phys. Rev. B* **82** 094116

[9] Liu C X, Qi X L, Zhang H, Dai X, Fang Z and Zhang S C 2010 *Phys. Rev. B* **82** 045122

[10] Parlinski K, Li Z Q and Kawazoe Y 1997 *Phys. Rev. Lett.* **78** 4063

[11] Togo A, Oba F and Tanaka I 2008 *Phys. Rev. B* **78** 134106